Disulfide locking a sodium channel voltage sensor reveals ion pair formation during activation

Paul G. DeCaen, Vladimir Yarov-Yarovoy, Yong Zhao*, Todd Scheuer, and William A. Catterall†

Department of Pharmacology, University of Washington, Seattle, WA 98195-7280

Contributed by William A. Catterall, July 15, 2008 (sent for review June 4, 2008)

The S4 transmembrane segments of voltage-gated ion channels move outward on depolarization, initiating a conformational change that opens the pore, but the mechanism of S4 movement is unresolved. One structural model predicts sequential formation of ion pairs between the S4 gating charges and negative charges in neighboring S2 and S3 transmembrane segments during gating. Here, we show that paired cysteine substitutions for the third gating charge (R3) in S4 and D60 in S2 of the bacterial sodium channel NaChBac form a disulfide bond during activation, thus "locking" the S4 segment and inducing slow inactivation of the channel. Disulfide locking closely followed the kinetics and voltage dependence of activation and was reversed by hyperpolarization. Activation of D60C:R3C channels is favored compared with single cysteine mutants, and mutant cycle analysis revealed strong free-energy coupling between these residues, further supporting interaction of R3 and D60 during gating. Our results demonstrate voltage-dependent formation of an ion pair during activation of the voltage sensor in real time and suggest that this interaction catalyzes S4 movement and channel activation.

voltage-sensing | gating charge | mutant cycle | sliding helix

Voltage-gated ion channels conduct electrical currents that are essential for a wide range of physiological processes including neuronal excitation, action potential conduction, synaptic neurotransmission, and muscle contraction. In prokaryotes, ion channels are necessary for pH homeostasis, chemotaxis, and motility. Voltage-gated ion channels respond to changes in membrane potential by opening and closing ("gating") their ion-conducting pathway across the cell membrane. Gating is rapid, reversible, and steeply voltage-dependent, suggesting that charged gating particles associated with the channels move across the membrane in response to the electric field (1). Capacitative "gating currents" caused by these charge movements (2, 3) indicate that approximately 3–4 positive charges per voltage-sensing module move outward during gating of sodium or potassium channels (4–10). The primary structure of sodium channels (11) revealed four homologous domains containing six predicted alpha-helical segments (S1–S6) in each. Subsequently, the positively charged S4 segment was proposed to have a transmembrane position, serve as the voltage sensor that perceives changes in membrane potential, and move outward along a spiral path during channel activation to conduct the gating current and initiate a conformational change to open the pore (12, 13). A major thermodynamic obstacle to transmembrane movement of the S4 segment is stabilization of its positively charged amino acid residues in the membrane environment. The sliding helix model posits (12) that sequential formation of ion pairs with negatively charged amino acid residues in the S1, S2, and/or S3 segments serve to stabilize the S4 segments in the membrane and thereby catalyze their transmembrane movement. A detailed structural version of this gating model developed by using the Rosetta Membrane modeling method predicts sequential formation of specific ion pairs during gating (14, 15), but the rapid, state-dependent formation of ion pairs predicted in this gating model has not been experimentally tested.

The conserved positively charged arginine residues (R1–R4), positioned at three-residue intervals in the S4 segments of sodium and potassium channels, and a negatively charged residue in the S2 segment contribute to gating charge transfer (4, 7, 9). The S4 segments have been shown to move outward during voltage-dependent activation in voltage clamp, covalent labeling, and fluorescence imaging experiments (16–20). Interactions between the positively charged residues in the S4 segments and negatively charged residues in the S2 and S3 segments are important for cell surface expression of potassium channels (21), suggesting that electrostatic interactions between these transmembrane segments are necessary for proper protein folding. However, it is not known whether ion pairs between amino acid residues in the S2 and S4 segments are formed on the millisecond time scale during voltage-dependent gating and thereby catalyze the transmembrane movement of the S4 gating charges.

	S2 TM	S4 TM
NaChBac	YRI**D**LVLLWIFTIEIAMRFLA	VL**R**IL**R**VL**R**VL**R**AISVVP
K_vAP	YLV**D**LILVIILWADYAYRAYK	LF**R**LV**R**LL**R**FL**R**ILLIIS
K_v1.2	FIV**E**TLCIIWFSFEFLVRFFA	IL**R**VI**R**LV**R**VF**R**IFKLSR
Na_v1.2 I	KNV**E**YTFTGIYTFESLIKILA	AL**R**TF**R**VL**R**AL**K**TISVIP
II	SVG**N**LVFTGIFTAEMFLKIIA	VL**R**SF**R**LL**R**VF**K**LAKSWP
III	EYA**D**KVFTYIFILEMLLKWVA	SL**R**TL**R**AL**R**PL**R**ALSRFE
IV	YWI**N**LVFIVLFTGECVLKLIS	VI**R**LA**R**IG**R**IL**R**LIKGAK

Scheme 1. Positions of S2 and S4 gating charges are conserved in NaChBac

The bacterial sodium channel NaChBac of *Bacillus halodurans* (22) is a small, 274-residue homotetrameric channel, which is a likely ancestor of the larger (≈2,000 residue) eukaryotic sodium and calcium channels that contain four covalently linked homologous domains. Despite its structural simplicity, NaChBac resembles individual domains of sodium and calcium channels having six transmembrane segments with a voltage-sensing module consisting of S1–S4 segments and a pore-forming module of S5 and S6 segments (22). Its activation is steeply voltage-dependent, but its kinetics of activation and inactivation are slower than eukaryotic sodium channels (6, 22). Its relatively small size and homotetrameric structure make it an ideal model for analysis of the molecular mechanisms of voltage-dependent gating.

Disulfide bond formation between substituted cysteine residues has proven to be a powerful tool to analyze the structures of intermediates in protein-folding reactions (23, 24). Such disulfide bonds between substituted cysteine residues have been shown to lock intermediates in protein-folding pathways (23). Here, we have adapted this method to analyze the interaction of R3 in the S4

Author contributions: P.G.D., V.Y.-Y., Y.Z., T.S., and W.A.C. designed research; P.G.D. and V.Y.-Y. performed research; P.G.D., V.Y.-Y., and Y.Z. contributed new reagents/analytic tools; P.G.D., V.Y.-Y., T.S., and W.A.C. analyzed data; and P.G.D., V.Y.-Y., T.S., and W.A.C. wrote the paper.

The authors declare no conflict of interest.

*Present address: Cerep Inc., 15318 NE 95th Street, Redmond, WA 98052.

†To whom correspondence should be addressed. E-mail: wcatt@u.washington.edu.

This article contains supporting information online at www.pnas.org/cgi/content/full/0806486105/DCSupplemental.

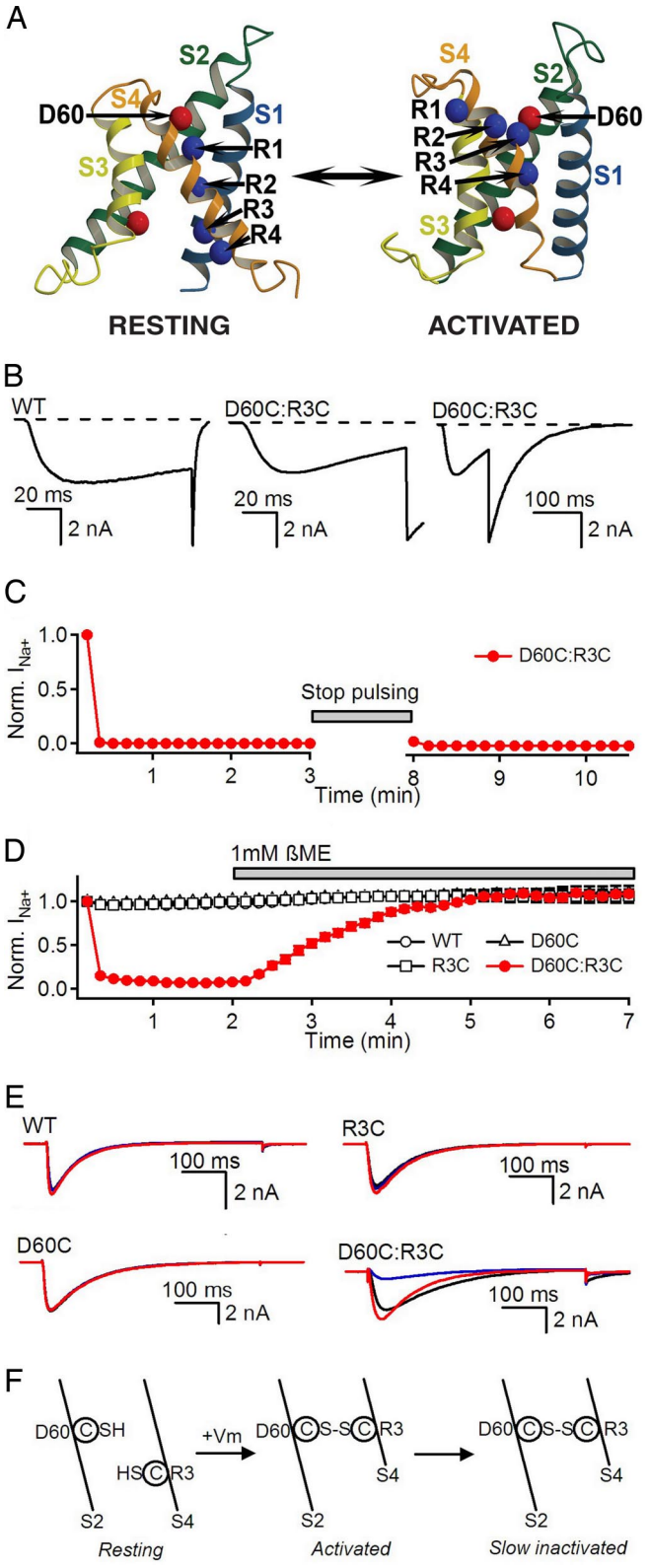

Fig. 1. Disulfide locking and recovery of D60C:R3C. (*A*) Rosetta-Membrane model. View of the ribbon representation of the voltage-sensing module of NaChBac in the resting (*Left*) and activated (*Right*) states. Segments S1 through S4 are colored individually and labeled. Side chains of gating-charge-carrying arginines in S4 (labeled R1 through R4 and colored blue) and D60 and E70 in S2 (colored red) are represented as spheres. (*B*) NaChBac WT and D60C:R3C current traces elicited by depolarizations to 0 mV for 100 ms followed by return to the holding potential of −120 mV. (*C*) Mean normalized peak currents elicited by 0.1 Hz trains of 500-ms depolarizations to 0 mV from a holding potential of −140 mV in tsA-201 cells expressing NaChBac D60C:R3C channels ($n = 7$). After 3 min, the pulsing was stopped for 5 min to test for channel recovery. (*D*) Mean normalized peak currents elicited by a 0.1 Hz train of 500-ms depolarizations to 0 mV from a holding potential of −140 mV in tsA cells transfected with −201 WT D60C, R3C, or D60C:R3C channels ($n = 8$). After 2 min in the control saline conditions, cells were exposed to 1 mM βME. (*E*) Current traces from indicated NaChBac constructs from the experiment described in *D*. Black traces are from the first depolarizing pulse of the experiment ($t = 0$ min.). Blue traces are from the last pulse before exposure to βME ($t = 2$ min). Red traces are after 5 min of βME treatment ($t = 7$ min). (*F*) Scheme representing the proposed state-dependent interaction of the cysteine residues followed by slow inactivation.

segment of NaChBac with D60 in the S2 segment in real-time voltage clamp experiments by measurements of state-dependent disulfide locking of substituted cysteine residues. Our results with this technique demonstrate a rapid, state-dependent interaction between these residues during voltage-dependent activation and suggest an important role for this interaction in catalyzing the transmembrane movement of the S4 gating charges.

Results and Discussion

Disulfide Locking of the NaChBac Voltage Sensor. In NaChBac, the first four arginine gating charges of the S4 transmembrane segment are in equivalent positions to those in the voltage-sensing modules in most mammalian voltage-gated ion channels (Scheme 1, residues indicated in bold).

In addition, the first negative charge in the S2 segment of NaChBac (D60) is in an analogous position to negatively charged aspartate or glutamate residues or hydrophilic asparagine residues that have a partially negatively charged carbonyl group in other voltage-gated sodium and potassium channels (Scheme 1). We developed a structural model for activation of the voltage sensor of NaChBac by using the Rosetta-Membrane algorithm, and the approach we described for $K_V1.2$ channels (15). The model is based on the X-ray structure of the activated state of $K_v1.2$ (25), *ab initio* modeling of $K_v1.2$ in its resting and activated states (14, 15), and extension of those methods to NaChBac. In the resting state, the first arginine gating charge (R1) of the S4 segment is predicted to interact with D60 in the S2 segment [Fig. 1*A* and supporting information (SI) *Text*]. On activation of the voltage sensor, the model predicts that the S4 segment moves outward along a spiral pathway, and the third arginine gating charge (R3) moves into close proximity to D60 in the S2 segment in its activated state (Fig. 1*A*). These sequential ion pair interactions are an essential feature of the sliding helix gating mechanism (12, 13), in which they serve to stabilize and catalyze the transmembrane movement of the S4 segment.

To test this predicted interaction, we generated NaChBac cDNA constructs containing single and double cysteine substitutions for R3 in the S4 segment and D60 in the S2 segment (D60C, R3C, and D60C:R3C). Because NaChBac is a cysteineless protein, any functional effects caused by disulfide linkage can be attributed to formation of R3C:D60C disulfide bonds. We hypothesized that the two sulfhydryls of the substituted cysteines would interact on channel activation, as predicted by our model (Fig. 1*A*), form a disulfide bond, and lock the voltage sensor in a fixed position. The cDNA constructs encoding WT and mutant NaChBac channels were transfected into tsA-201 cells, and the transfected cells were analyzed by whole-cell voltage clamp recording to test for functional effects of disulfide locking. Activation of D60C:R3C channels by a single depolarization from −120 mV to 0 mV for 100 ms resulted in activation of sodium current for WT and D60C:R3C channels (Fig. 1*B Left* and *Center*). Repolarization of WT channels resulted in a rapidly decaying tail current that reflects the rapid closure of the channels (Fig. 1*B Left*). In contrast, this rapid tail current is completely lost in D60C:R3C channels (Fig. 1*B Center*), indicating

that they are stabilized in the activated state. The current conducted by D60C:R3C channels decays completely but much more slowly (Fig. 1*B Right*), which reflects slow inactivation of the disulfide-locked channels (see next section and Fig. 2).

Despite the apparent prolonged activation of D60C:R3C channels, a single depolarization resulted in a total loss of I_{Na} in subsequent depolarizations, which did not recover after 5 min at −120 mV (Fig. 1*C*). In contrast, I_{Na} for WT NaChBac and the two single mutants, R3C and D60C, were unaffected by the repetitive pulsing protocol (Fig. 1*D*). Loss of I_{Na} for the double mutant D60C:R3C, but not for the corresponding single mutants D60C and R3C, also suggests that these two substituted cysteine residues interact and form a disulfide bond during the first 500-ms depolarizing pulse and lock the voltage sensor.

To test whether the loss of I_{Na} observed for D60C:R3C is indeed caused by disulfide bond formation, we perfused the sulfhydryl reagent β-mercaptoethanol (βME) onto cells after disulfide locking the D60C:R3C channels (Fig. 1 *D* and *E*). In the presence of βME, I_{Na} recovered to the initial current magnitude within 3 min. Based on these results, we conclude that the loss of I_{Na} is caused by disulfide locking of the S4 voltage sensor in an activated conformation. Like eukaryotic sodium and calcium channels, NaChBac channels enter a slow-inactivated state after activation (22). Therefore, disulfide locking of the voltage sensor in an activated state would cause the NaChBac channels to enter the slow-inactivated state, from which they are unable to recover on membrane repolarization to −120 mV because of disulfide locking (Fig. 1*F*).

Voltage-Dependent Reversal of Disulfide Locking. Disulfide bonds in proteins have a free energy of ≈2–5 kcal/mol (26, 27). The electrical free energy gained by movement of an S4 voltage sensor with three positive charges through an electrical potential of −200 mV is 13.8 kcal/mol (see *SI Text* for calculations of the energy and force of voltage sensor movement). Therefore, we hypothesized that a hyperpolarizing pulse to −200 mV would have sufficient energy to break the disulfide bond formed between the S2 and S4 segments and release the disulfide-locked voltage sensor. To test this hypothesis, we hyperpolarized disulfide-locked D60C:R3C channels to increasingly negative membrane potentials and then depolarized to measure the recovery of I_{Na}. Under control conditions, hyperpolarization to potentials more negative than −150 mV caused progressive recovery of I_{Na} (Fig. 2*A*). If this voltage-dependent reversal of disulfide-locking requires reduction of the disulfide bond between R3 and D60, the recovery of I_{Na} should be enhanced by treatment with βME. As expected, in the presence of 1 mM βME, the recovery of I_{Na} is substantially shifted to more positive membrane potentials (Fig. 2*A*). Comparison of the recovery of I_{Na} after disulfide locking in the absence and presence of βME reveals that the energy required for reversal is much less, as reflected in the positive shift of $V_{1/2}$ from −196 mV in control to −168 mV in the presence of βME and by the steeper slope. These results indicate that the electrical energy required for the reversal of disulfide locking by hyperpolarization is substantially reduced by a sulfhydryl reagent that prevents formation of disulfide bonds.

We also compared the rate of recovery of I_{Na} during hyperpolarization to −160 mV in control conditions and in the presence of βME. The rate was at most slightly increased by βME (control, τ = 12 ± 3 s; βME, τ = 9.5 ± 1 s), but the peak sodium current was substantially larger after βME treatment (Fig. 2*B*). These results indicate that voltage-dependent reversal of disulfide locking is not substantially accelerated by βME, but the extent of reversal of disulfide locking is increased because of re-formation of the disulfide bond is impaired by the reducing agent.

The rate of loss of NaChBac current after disulfide locking is similar to the rate of slow inactivation of NaChBac (Fig. 1). For example, after a depolarization +20 mV more positive than half-maximal activation (−30 mV for D60C:R3C; −20 mV for WT), the time constant for the decay of the Na^+ current of disulfide-locked

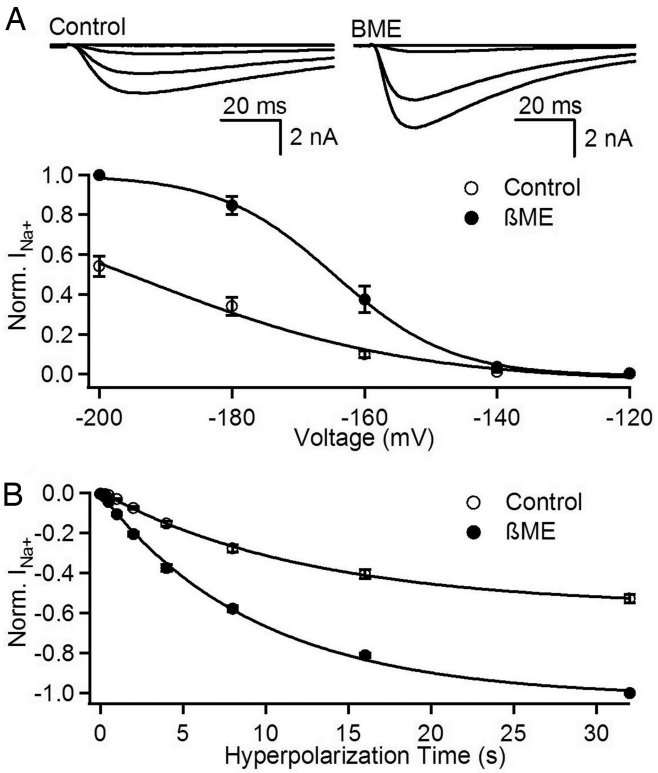

Fig. 2. Reversal of disulfide locking by hyperpolarization and βME. (*A*) Voltage-dependence of reversal of disulfide locking. (*Top*) Families of D60C:R3C currents elicited by 100-ms depolarizations to 0 mV after 5-s hyperpolarizing pulses ranging from −200 mV to −120 mV in control and in the presence of 1 mM βME (n = 8). Before each trial, channels were subjected to five 500-ms pulses to 0 mV to disulfide-lock and fully inactivate all voltage sensors (data not shown). (*Bottom*) For each cell, peak currents were normalized to the largest peak current in the presence of βME. Mean normalized peak currents were replotted against the potential of the hyperpolarizing prepulse. (*B*) Time dependence of reversal of disulfide locking. Fully locked and inactivated D60C:R3C channels (see above) were hyperpolarized to −160 mV for the indicated times followed by a 100-ms test pulse to 0 mV in control conditions or in the presence of 1 mM βME. (n = 7). For each cell, peak test pulse currents were normalized to the peak current after the 32-s hyperpolarization in the presence of βME. Mean normalized peak currents (±SEM) are plotted against prepulse duration.

D60C:R3C channels (τ = 90 ± 8 ms; n = 8) is similar to the time constant for slow inactivation of WT (τ = 120 ± 13 ms; n = 9). The small difference between these values may reflect the incomplete compensation for the more negative voltage dependence of activation of the double mutant. The similarity of these kinetics is consistent with the conclusion that loss of Na^+ current for the disulfide-locked D60C:R3C channels reflects slow inactivation. This conclusion is also supported by recovery of Na^+ current by hyperpolarization (Fig. 2). Evidently, disulfide locking D60C with R3C favors slow inactivation, suggesting that this disulfide-locked conformation of the voltage sensor is effective in initiating the slow-inactivation process, and that the slow-inactivation process can proceed with the S4 voltage sensor locked in place.

Kinetics of Activation, Disulfide Locking, and Inactivation. The ability to reverse disulfide locking by hyperpolarization allowed us to design experiments to measure the kinetics of disulfide locking of D60C:R3C channels. After a prepulse to −160 mV for 5 s, we measured the onset of disulfide locking of D60C:R3C that was irreversible at −120 mV and compared it to the time course of activation and inactivation of I_{Na}. For D60C:R3C, depolarization to −30 mV for the indicated prepulse durations caused progressive

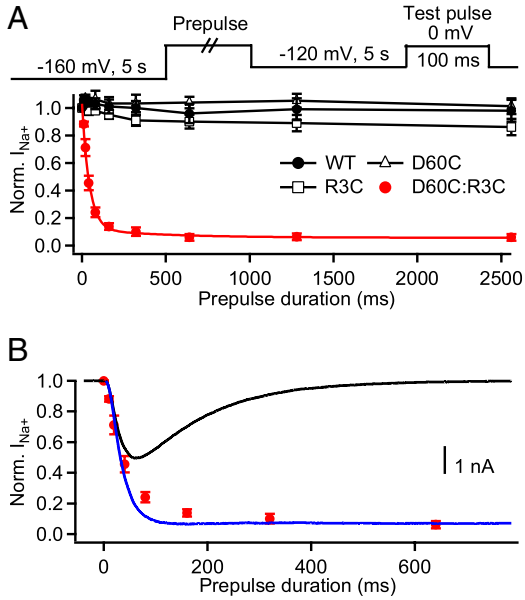

Fig. 3. Time course of voltage-sensor locking. (*A*) Rate of prepulse-dependent inactivation of D60C:R3C channels. D60C:R3C channels were first unlocked by a 5-s prepulse to −160 mV. Cells were then depolarized for the indicated times to $\approx V_{1/2}$ + 20 mV (WT, −20 mV; D60C and R3C, 0 mV; and D60C:R3C, −30 mV), returned to −120 mV for 5 s, and depolarized 100-ms test pulse to 0 mV. Peak test pulse current at 0 mV was normalized to the control with a test pulse current in the absence of a prepulse, and mean (±SEM) was plotted versus prepulse duration (n = 6). (*B*) Comparison of the rates of disulfide locking and activation. Sodium current recorded during a −30 mV prepulse (black curve). The time course of activation in the absence of inactivation (blue trace) was estimated by fitting an exponential to the current decay and adding the inactivated component back to the total current. This time course of activation is compared with the rate of loss of test pulse current (red circles) from *A*.

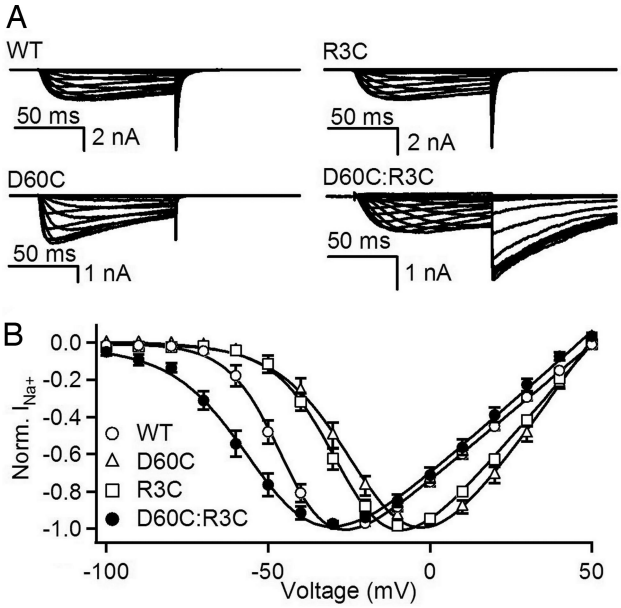

C

Channel	Z	$V_{1/2}$	ΔG°	ΔΔG°	ΣΔG°
Wt	3.8 ±0.1	-43 ±2	-3.9 ±0.2	-	-
D60C	2.6 ±0.2	-19 ±3	-1.2 ±0.2	2.67	-
R3C	3.1 ±0.1	-26 ±2	-1.9 ±0.2	1.97	-
D60C:R3C	2.4 ±0.1	-50 ±3	-2.8 ±0.3	1.11	3.53

Fig. 4. Mutant cycle analysis of coupling between NaChBac D60C and R3C mutations. (*A*) Families of sodium current traces from each of the indicated NaChBac channels activated by 100-ms depolarizations to potentials ranging from −120 mV to −50 mV in 10 mV increments from a holding potential of −160 mV. (*B*) Normalized peak currents during depolarizations to the indicated potentials (n = 10; ±SEM). (*C*) Mutant cycle analysis. Estimated values for Z and $V_{1/2}$ in mV, $\Delta G°$, $\Delta\Delta G°$, and $\Sigma\Delta G°$ in kcal/mol obtained by fitting the I/V relationships for the WT and mutant NaChBac channels are presented (see *Materials and Methods*).

disulfide locking and loss of I_{Na} that was >90% complete by 300 ms (Fig. 3*A*, see examples of I_{Na} traces in Fig. S1). In contrast, no loss of current was observed for WT NaChBac or the single mutants (Fig. 3*A*). Therefore, the rapid loss of I_{Na} reflects disulfide locking of the S2 and S4 segments. This rapid initial rate of loss of I_{Na} caused by disulfide locking was similar to the rate of channel activation (Fig. 3*B*). At the first three time points, there is a close quantitative correlation between the rate of activation (black curve) and the extent of disulfide locking (red points), but the two diverge as I_{Na} inactivates (Fig. 3*B*). To compare the time course of disulfide locking to the time course of activation without interference from inactivation, we estimated the time course of activation of I_{Na} alone (blue line) by subtracting the effect of inactivation determined from a fit to a single exponential function. Comparison of the time course of disulfide locking to activation reveals nearly identical kinetics. These results indicate that disulfide locking occurs nearly immediately after activation on the millisecond time scale.

Mutant Cycle Analysis of the Voltage Dependence of Activation of NaChBac Channels. Our results on disulfide locking indicate that R3 and D60 in NaChBac interact with each other during voltage-dependent activation. To test this interaction with an independent approach, we used mutant cycle analysis (28) to assess the energy of association of these amino acid residues during activation of NaChBac channels. We measured the voltage dependence of activation of WT, single-mutant, and D60C:R3C double-mutant channels from current-voltage (I/V) relationships after a prepulse to −160 mV (Fig. 4*A*). The single mutations D60C and R3C shifted the $V_{1/2}$ for activation 17 to 24 mV to more positive membrane potentials, indicating that the single mutations oppose activation of NaChBac channels (WT, $V_{1/2}$ = −43 ± 2 mV; D60C, $V_{1/2}$ = −19 ± 3 mV; R3C $V_{1/2}$ = −26 ± 2 mV; n = 10) (Fig. 4*A*). Evidently, mutation of charged amino acid residues results in channels that are more difficult to activate, similar to reports (29–31). The increases in energy required to activate these single-mutant channels compared with WT channels are similar (ΔΔG° = 1.97 to 2.67 kcal/mol) (Fig. 4*C*), consistent with the hypothesis that the same interaction is disrupted by each single mutation.

We measured activation of the double-mutant D60C:R3C channels by using the same protocol as for WT and single-mutant channels. In contrast to the positive shifts in the I/V relationships of the single-mutant channels, the paired mutations facilitate activation by negatively shifting $V_{1/2}$ by −7 mV relative to WT (D60C:R3C $V_{1/2}$ = −50 ± 3 mV, n = 10) (Fig. 4*A*). These results indicate that formation of the D60C:R3C disulfide bond stabilizes the voltage sensor in its outward, activated position and thereby enhances voltage-dependent activation, whereas disruption of normal ion pair formation between D60 and R3 in the single mutants D60C and R3C opposes activation.

To analyze the free-energy coupling between D60C and R3C quantitatively, we applied mutant cycle analysis as in previous studies of ion channels (32–35). For mutations whose effects on the energetics of gating are independent, the free-energy changes

caused by the two single mutations will be additive; their sum will equal the free-energy change caused by the double mutation, and the coupling energy, calculated as the difference between these two values, will be zero. In contrast, if the mutated amino acid residues interact, the effects of their mutations will not be independent, and the free energy changes will not be additive, resulting in a coupling energy that is significantly > or < zero. Our mutations are clearly not independent because the two single mutations positively shift the voltage dependence of activation, whereas the double mutation negatively shifts the voltage dependence of activation. Comparison of the free energies ($\Delta G°$) required to open the single-mutant and double-mutant channels, relative to the WT channels, gives values for $\Delta\Delta G°$, which reflect the relative free energies for activation of the three mutants. Calculation of the coupling free energy ($\Sigma\Delta G°$) from the four values for $\Delta G°$ yields a value of 3.5 kcal/mol (Fig. 4*C* and *Materials and Methods*). This large coupling energy indicates that D60C and R3C interact with each other during gating. The coupling energy is in the range of the free energy of disulfide bond formation, consistent with our conclusion that these residues form a disulfide bond during voltage-dependent activation.

Disulfide Locking and Ion Pair Formation in the NaChBac Voltage Sensor. The Rosetta sliding helix model of voltage-dependent gating (15) (Fig. 1*A*) proposes that the four S4 gating charges of NaChBac interact sequentially with D60 in the S2 segment during voltage-dependent gating, which catalyzes the transmembrane movement of the S4 segment. Our results provide strong support for formation of an ion pair between D60 in the S2 segment and R3 in the S4 segment. Cysteine residues substituted for D60 and R3 interact with each other during voltage-dependent gating and form a disulfide bond that locks the voltage sensor in an activated position and drives the channel irreversibly into the slow-inactivated state. The rate and voltage dependence of disulfide locking closely follows the rate and voltage dependence of channel activation. Disulfide locking is reversed by strong hyperpolarization and treatment with βME. The state dependence of disulfide locking and the close correlation with the kinetics and voltage dependence of channel activation indicate that R3 moves into close contact with D60 during the activation process and forms a disulfide bond almost immediately.

Disulfide bond formation between substituted cysteine residues is a well established method of analysis of the intermediates in protein folding (23, 24). Because the reactive sulfhydryls must approach within 2 Å at the time of formation a disulfide bond, this is a high-resolution method of analysis of intraprotein interactions. The main caveat for this method of structure-function analysis is the possibility that disulfide bond formation may stabilize a rare conformation of the protein of interest. This is a major concern when disulfide bond formation is slow, allowing conformational states that are only occasionally visited to become disulfide locked in place. Our results exclude this possibility because we find that disulfide locking takes place within milliseconds of activation. Therefore, these results provide strong support for the formation of an ion pair between D60 and R3 during normal NaChBac gating.

These conclusions from disulfide-locking experiments were confirmed by mutant cycle analysis. By analysis of WT, single-mutant, and double-mutant channels, we found that D60C and R3C interact with each with a coupling energy of 3.5 kcal/mol, within the range of known disulfide bonds in proteins. These results provide additional support for interaction of D60 with R3 during NaChBac gating and confirm that the disulfide locking of substituted cysteine residues gives an accurate picture of the interactions between these two residues during activation.

Ion Pair Formation in Real Time During Voltage Sensor Activation. A primary question about voltage sensor function is: What chemical interactions allow the highly charged S4 segment to move across the membrane? Formation of ion pairs between gating-charge-carrying arginine residues and negatively charged amino acid residues in neighboring transmembrane segments is an essential feature of the sliding helix model of voltage dependent gating (12, 13), in which sequential charge–charge interactions serve to stabilize the S4 segment in the membrane environment and catalyze its transmembrane movement. Our results provide experimental evidence for ion pair formation in real time during activation of a voltage sensor and therefore are consistent with this mechanism.

Alternative gating models are also compatible with our results and can incorporate ion pair formation as part of the mechanism for the catalysis of movement of the S4 segment. The "paddle" gating mechanism envisions a sweeping paddle-like motion of the S3-S4 helical hairpin (the gating paddle) across the phospholipid bilayer from a position lying nearly horizontal along the inner surface of the membrane to a transmembrane position (36). Phospholipid head groups are proposed to provide stabilizing interactions for this movement of the gating charges (37), but it would also be possible for ion pair interactions between S2 and S4 segments to form as a result of this paddle motion and contribute to catalyzing the outward movement of the voltage sensor. The "transporter" model of gating posits that the transmembrane movement of the S4 segment is small, whereas the surrounding S1, S2, and S3 segment rearrange to change the accessibility of the gating charges from internal to external (38). The Rosetta-Membrane structural version of the sliding helix model also incorporates this feature in that the outward spiral movement of the S4 helical segment is accompanied by a counter-rotation of the S1 through S3 helical segments (14, 15). Although the transporter model of gating does not include ion pair interactions between the R3 gating charge and the negatively charged residues in the S2 segment, the movement of the voltage sensor postulated in this model could also include formation of an ion pair interaction in an intermediate state or in the final open state. Thus, although our experimental approach was developed with reference to the sliding-helix gating model, ion pair formation during activation of the voltage sensor is a model-independent mechanism that may contribute to the stabilization of the S4 segment in the transmembrane environment and catalysis of its outward movement in any of the current models of voltage sensor function. Ion pair formation during activation, as demonstrated here, is therefore a crucial element that must be included in the mechanism of voltage sensing and gating of ion channels.

Materials and Methods

Electrophysiology. Whole-cell voltage-clamp experiments were performed at 22°C on transiently transfected tsA-201 cells as described (39). Cells were seeded onto glass coverslips and placed in a perfusion chamber for experiments where reducing agents were used. Otherwise, all other experiments were recorded from cells seeded in tissue culture dishes. The extracellular solution contained (in mM) NaCl (150), $CaCl_2$ (1.5), $MgCl_2$ (1), KCl (2), glucose (10), and Hepes (10) (pH 7.4), and the intracellular (pipette) solution contained (in mM) CsF (105), EGTA (10), NaCl (35), Mg-ATP (4), and Hepes (10) (pH 7.5). βME was added to the extracellular solution to a final concentration of 1 mM within 1 h of use. For experiments using βME, cells were continuously perfused with extracellular solution (1–2 ml/min). The steady-state effect for reversal of disulfide locked D60C:R3C channels was achieved after 3–5 min of βME exposure and was monitored by I_{Na}^+ recovery during 500-ms pulses to 0 mV at 0.1 Hz from a holding potential of −140 mV. In experiments where D60C:R3C channels were tested, residual linear leak and capacitance were subtracted offline in IGOR 6.00 (Wavemetrics) by measuring leak and capacitive current from disulfide-locked/inactivated channel pulses and integrating to the test pulse. Data were analyzed using Igor Pro 6.00. The voltage dependence of activation was characterized by using fits of $(V-V_{Rev})/\{1+\exp[(V-V_{1/2})/k]\}$ to current-voltage relationships, where V_{Rev} is the extrapolated reversal potential, $V_{1/2}$ is the half-activation voltage, and k is a slope factor equal to RT/ZF; Z is the apparent gating charge and F is Faraday's number. Half-inactivation

voltages were derived from fits of a Boltzmann function, $1/[1+\exp(V-V_{1/2})/k]$, to steady-state inactivation curves. Double exponential decay of inactivating currents were fit with the following equation: $C + A_1(e^{-t/\tau 1}) + A_2(e^{-t/\tau 2})$ where τ_1 and τ_2 were the time constants of each exponential component, A_1 and A_2 are their respective amplitudes, and C was the baseline.

Thermodynamic Mutant Cycle Analysis. The parameter Z was determined from fits to current-voltage relationships as described above. The amount of free energy required to shift the channel from the open to closed state was calculated as $\Delta G°_{O\rightarrow C}$ (kcal/mol) $= -23.06ZFV_{½}$, where F is Faraday's number and $V_{1/2}$ is the half-activation voltage. The perturbation in free energy of the mutant channel relative to the WT was calculated as $\Delta\Delta G° = \Delta(ZFV_{½}) = -F(Z_{mut}V_{1/2mut} - Z_{wt}V_{1/2wt})$. Coupling of nonadditive free energy was calculated as $\Sigma\Delta G°_{coupled} = [(\Delta G°_{D60C} - \Delta G°_{wt}) - (\Delta G°_{D60C:R3C} - \Delta G°_{R3C})]$ (35).

ACKNOWLEDGMENTS. We thank Ms. Elizabeth Sharp for excellent technical assistance in molecular biology. This work was supported by National Institutes of Health Research Grant R01NS15751 (to W.A.C.) and Grant K01MH6725 (to V.Y.-Y.) and a National Research Service Award from NIH Training Grant T32GM07270 (to P.G.D.).

1. Hodgkin AL, Huxley AF (1952) A quantitative description of membrane current and its application to conduction and excitation in nerve. *J Physiol* 117:500–544.
2. Armstrong CM, Bezanilla F (1973) Currents related to movement of the gating particles of the sodium channels. *Nature* 242:459–461.
3. Keynes RD, Rojas E (1974) Kinetics and steady-state properties of the charged system controlling sodium conductance in the squid giant axon. *J Physiol* 239:393–434.
4. Seoh SA, Sigg D, Papazian DM, Bezanilla F (1996) Voltage-sensing residues in the S2 and S4 segments of the Shaker K^+ channel. *Neuron* 16:1159–1167.
5. Tombola F, Pathak MM, Isacoff EY (2006) How does voltage open an ion channel? *Annu Rev Cell Dev Biol* 22:23–52.
6. Kuzmenkin A, Bezanilla F, Correa AM (2004) Gating of the bacterial sodium channel, NaChBac: Voltage-dependent charge movement and gating currents. *J Gen Physiol* 124:349–356.
7. Aggarwal SK, MacKinnon R (1996) Contribution of the S4 segment to gating charge in the *Shaker* K^+ channel. *Neuron* 16:1169–1177.
8. Zagotta WN, Aldrich RW (1990) Voltage-dependent gating of Shaker A-type potassium channels in Drosophila muscle. *J Gen Physiol* 95:29–60.
9. Schoppa NE, McCormack K, Tanouye MA, Sigworth FJ (1992) The size of gating charge in WT and mutant *Shaker* potassium channels. *Science* 255:1712–1715.
10. Hirschberg B, Rovner A, Lieberman M, Patlak J (1995) Transfer of twelve charges is needed to open skeletal muscle Na^+ channels. *J Gen Physiol* 106:1053–1068.
11. Numa S, Noda M (1986) Molecular structure of sodium channels. *Ann NY Acad Sci* 479:338–355.
12. Catterall WA (1986) Molecular properties of voltage-sensitive sodium channels. *Annu Rev Biochem* 55:953–985.
13. Guy HR, Seetharamulu P (1986) Molecular model of the action potential sodium channel. *Proc Natl Acad Sci USA* 508:508–512.
14. Yarov-Yarovoy V, Baker D, Catterall WA (2006) Voltage sensor conformations in the open and closed states in ROSETTA structural models of K^+ channels. *Proc Natl Acad Sci USA* 103:7292–7297.
15. Pathak MM, *et al.* (2007) Closing in on the resting state of the Shaker K^+ channel. *Neuron* 56:124–140.
16. Kontis KJ, Goldin AL (1997) Sodium channel inactivation is altered by substitution of voltage sensor positive charges. *J Gen Physiol* 110:403–413.
17. Cha A, Bezanilla F (1997) Characterizing voltage-dependent conformational changes in the Shaker K^+ channel with fluorescence. *Neuron* 19:1127–1140.
18. Larsson HP, Baker OS, Dhillon DS, Isacoff EY (1996) Transmembrane movement of the Shaker K^+ channel S4. *Neuron* 16:387–397.
19. Yang N, Horn R (1995) Evidence for voltage-dependent S4 movement in sodium channel. *Neuron* 15:213–218.
20. Yang N, George AL, Jr., Horn R (1996) Molecular basis of charge movement in voltage-gated sodium channels. *Neuron* 16:113–122.
21. Papazian DM, *et al.* (1995) Electrostatic interactions of S4 voltage sensor in Shaker K^+ channel. *Neuron* 14:1293–1301.
22. Ren D, *et al.* (2001) A prokaryotic voltage-gated sodium channel. *Science* 294:2372–2375.
23. Clarke J, Fersht AR (1993) Engineered disulfide bonds as probes of the folding pathway of barnase: Increasing the stability of proteins against the rate of denaturation. *Biochemistry* 32:4322–4329.
24. Wahlberg E, Hard T (2006) Conformational stabilization of an engineered binding protein. *J Am Chem Soc* 128:7651–7660.
25. Long SB, Campbell EB, MacKinnon R (2005) Crystal structure of a mammalian voltage-dependent Shaker family K^+ channel. *Science* 309:897–903.
26. Siedler F, Rudolph-Bohner S, Doi M, Musiol HJ, Moroder L (1993) Redox potentials of active-site bis(cysteinyl) fragments of thiol-protein oxidoreductases. *Biochemistry* 32:7488–7495.
27. Schmidt B, Ho L, Hogg PJ (2006) Allosteric disulfide bonds. *Biochemistry* 45:7429–7433.
28. Serrano L, Horovitz A, Avron B, Bycroft M, Fersht AR (1990) Estimating the contribution of engineered surface electrostatic interactions to protein stability by using double-mutant cycles. *Biochemistry* 29:9343–9352.
29. Chahine M, Pilote S, Pouliot V, Takami H, Sato C (2004) Role of arginine residues on the S4 segment of the Bacillus halodurans Na^+ channel in voltage-sensing. *J Membr Biol* 201:9–24.
30. Blanchet J, Pilote S, Chahine M (2007) Acidic residues on the voltage-sensor domain determine the activation of the NaChBac sodium channel. *Biophys J* 92:3513–3523.
31. Zhao Y, Scheuer T, Catterall WA (2004) Reversed voltage-dependent gating of a bacterial sodium channel with proline substitutions in the S6 transmembrane segment. *Proc Natl Acad Sci USA* 101:17873–17878.
32. Hidalgo P, MacKinnon R (1995) Revealing the architecture of a K^+ channel pore through mutant cycles with a peptide inhibitor. *Science* 268:307.
33. McPhee JC, Ragsdale DS, Scheuer T, Catterall WA (1995) A critical role for transmembrane segment IVS6 of the sodium channel α subunit in fast inactivation. *J Biol Chem* 270:12025–12034.
34. Ranganathan R, Lewis JH, MacKinnon R (1996) Spatial localization of the K^+ channel selectivity filter by mutant cycle-based structure analysis. *Neuron* 16:131–139.
35. Yifrach O, MacKinnon R (2002) Energetics of pore opening in a voltage-gated K^+ channel. *Cell* 111:231–239.
36. Jiang Y, Ruta V, Chen J, Lee A, MacKinnon R (2003) The principle of gating charge movement in a voltage-dependent K^+ channel. *Nature* 423:42–48.
37. Schmidt D, Jiang QX, MacKinnon R (2006) Phospholipids and the origin of cationic gating charges in voltage sensors. *Nature* 444:775–779.
38. Chanda B, Asamoah OK, Blunck R, Roux B, Bezanilla F (2005) Gating charge displacement in voltage-gated ion channels involves limited transmembrane movement. *Nature* 436:852–856.
39. Qu Y, Rogers J, Tanada T, Scheuer T, Catterall WA (1995) Molecular determinants of drug access to the receptor site for antiarrhythmic drugs in the cardiac Na^+ channel. *Proc Natl Acad Sci USA* 270:25696–25701.